ADVANCED MATERIALS INTERFACES
Open Access

Supporting Information

for *Adv. Mater. Interfaces*, DOI 10.1002/admi.202300256

Adsorbate Formation/Removal and Plasma-Induced Evolution of Defects in Graphitic Materials

*Anna L. Eichhorn, Marvin Hoffer, Katharina Bitsch and Christian Dietz**

Supporting Information:

Adsorbate Formation/Removal and Plasma-Induced Evolution of Defects in Graphitic Materials

Anna L. Eichhorn[1], Marvin Hoffer[1], Katharina Bitsch, and Christian Dietz*

Physics of Surfaces, Institute of Materials Science, Technische Universität Darmstadt,
Alarich-Weiss-Str. 2, 64287 Darmstadt, Germany
[1]Anna L. Eichhorn and Marvin Hoffer equally contributed to the paper
Email: dietz@pos.tu-darmstadt.de
ORCID-IDs: A.L. Eichhorn: 0000-0003-1754-0276, C. Dietz: 0000-0002-4134-7516

1. Oxygen-Plasma Treatment of HOPG

According to Zandiatashbar *et al.* [1], the HOPG sample was placed on two glass slides for plasma treatment, as schematically shown in Figure S1b. Raman spectra have been acquired prior to and after plasma treatment for different durations of gas discharge from both, the exposed and the shielded side. This procedure was consecutively repeated in time intervals of 15 s. The peak intensity ratios I_D/I_G (red) and I_{2D}/I_G (blue) were obtained from the average of 80 Raman spectra acquired at different positions of the sample using an integration time of 5 s and were plotted against the cumulative plasma-treatment time. The results are shown in Figure S1, where open circles correspond to the data from the exposed area of three different HOPG samples and filled circles to the data from the shielded area determined on one of the three HOPG samples.

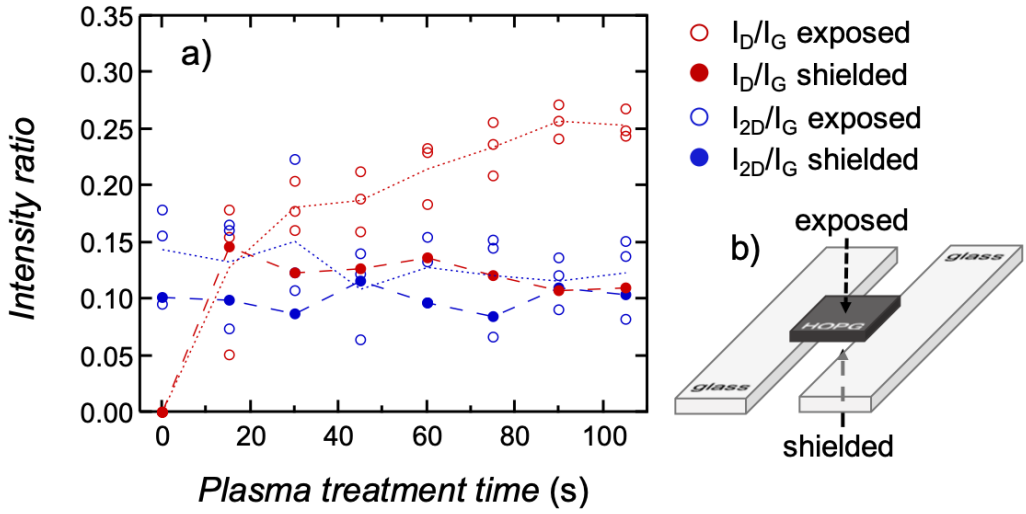

Figure S1: (a) Intensity ratios, derived from Raman spectroscopic measurements, as a function of the cumulative plasma treatment time for three HOPG samples (open circles). The intensity ratio between D- and G-peak is shown in red and between 2D- and G-peak in blue color. One HOPG sample was analyzed on both, the exposed (open circles) and the shielded area (filled circles), as schematically shown in (b).

From Figure S1a it becomes clear that, as it was expected, the intensity ratios I_{2D}/I_G (blue) are neither significantly influenced by the time nor by the type of plasma treatment, i.e. exposed (open circles) or shielded (filled circles). In contrast to that, it was shown that the ratio between the D- and the G-peak (red) depends on both, shielded/exposed plasma treatment and plasma-treatment time. Interestingly, after 15 s of plasma exposure, the ratio I_D/I_G (red) was similar for the exposed (open circles) and the shielded (filled circles) side of the HOPG sample. However, the ratio between D- and G-peak clearly differed for larger cumulative plasma-treatment times depending on shielded or exposed configuration. For the exposed configuration we observed an asymptotical increase of I_D/I_G reaching the saturation after approximately 90 s at 0.25 ± 0.05. For the shielded configuration the saturation was already reached after appoximately 15 s at 0.13 ± 0.02.

2. Adsorbate removal by oxygen-plasma treatment

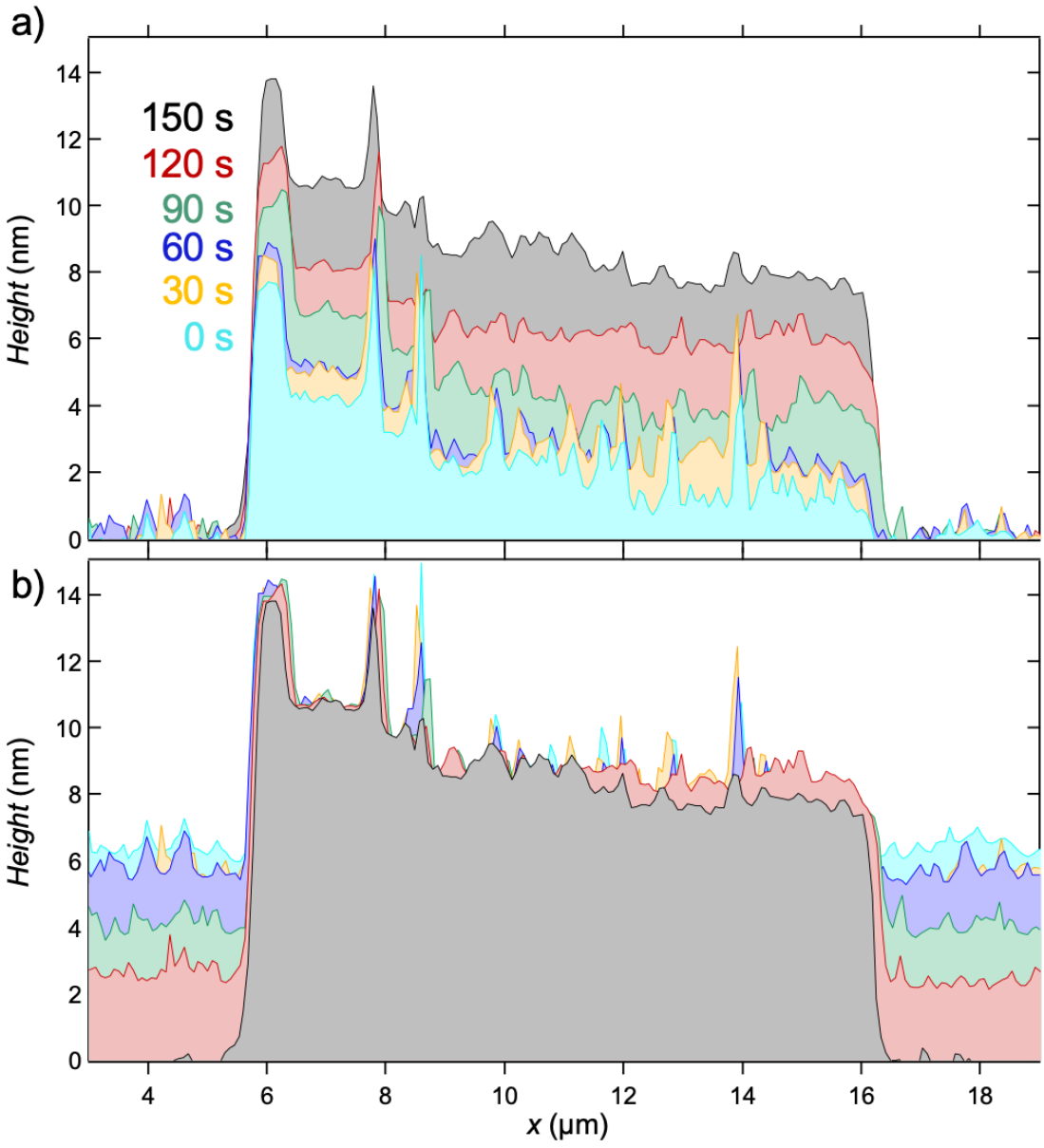

Figure S2: Adsorbate removal by oxygen-plasma treatment analyzed via cross-sections of AFM topography images. The sample was imaged prior to plasma treatment (light blue) and after 30 s (yellow), 60 s (blue), 90 s (green), 120 s (red), and 150 s (grey) of plasma treatment. For (a) the cross-sections aligned relative to the Si/SiO_2-substrate area and for (b) relative to the graphene/graphite sample area.

3. Raman intensity ratios as a function of graphene/graphite layer thickness

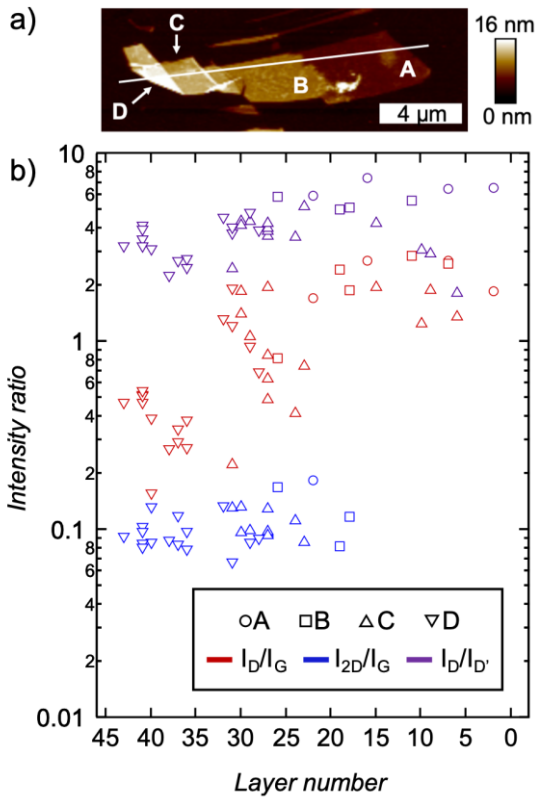

Figure S3: Raman intensity ratios measured within areas A (circle), B (square), C (tringle pointing up), and D (triangle pointing down), as marked in (a), as a function of layer number (b) resulting from stepwise oxygen-plasma treatment. The layer number was determined from cross-sections of AFM topography images, such as shown in Figure 1b (main text), where the height was divided by the graphene interlayer spacing (334.8 pm). The intensity ratio between D- and G-peak is shown in red, between 2D- and G-peak in blue and between D- and D'-peak in purple color.

4. Multifrequency AFM analysis of large-scale adsorbates and removal by oxygen-plasma treatment

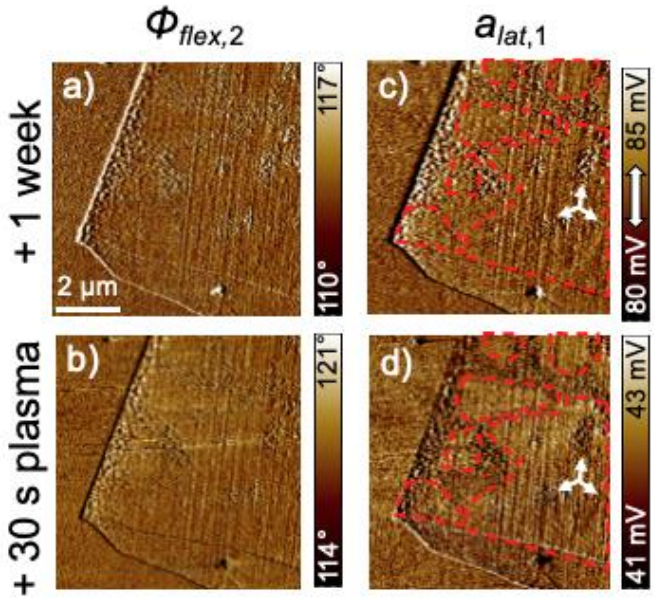

Figure S4: Adsorbate structure formation on a few-layer graphene/graphite flake analyzed after different durations of storage and oxygen-plasma treatment steps in AMFlex2-OLTor1-FMLat1 AFM mode. a–b: second flexural phase images and c–d: lateral drive amplitude images $A_{0\,(flex,2)}$ = 675 nm, $A_{flex,2}$ = 600 nm and $A_{lat,1}$= 1.766 nm. The white arrow within the color bar (c) indicates the direction of lateral oscillation. These AFM images represent a continuation of the storage and oxygen-plasma treatment steps of the AFM images shown in Figure 3 of the main text.

5. Graphene height and layer number evolution upon storage and plasma treatment

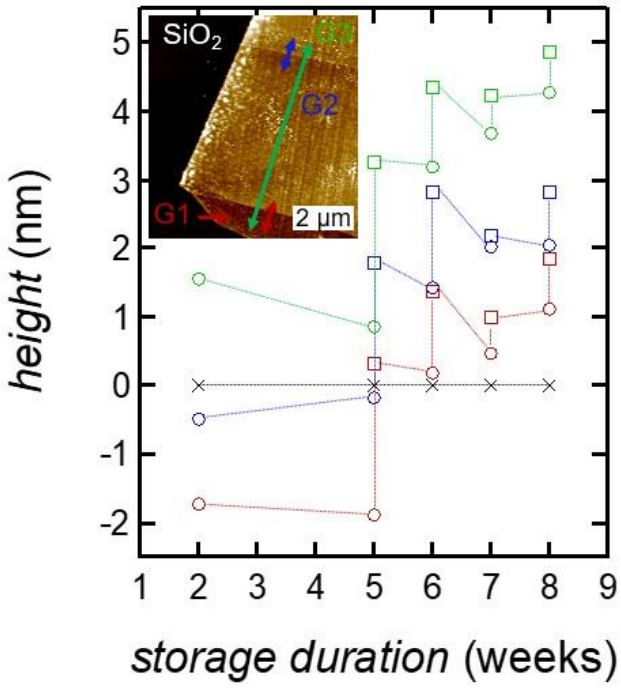

Figure S5: Height evolution of the investigated few-layer graphene/graphite flake upon storage in a polypropylene petri dish filled with laboratory air and plasma treatment extracted by using cross-sections in the recorded large-scale topographic images. The hollow circles represent the height values before and the hollow rectangles the values after each plasma treatment step. The black crosses represent the position of the silicon wafer substrate surface. The inset of Figure S5 shows an exemplary topography image of the examined few-layer graphene/graphite flake. The red colored double arrow indicates the layer number difference between G1 and G2, the green arrow the layer number difference between G1 and G3 and the blue one the layer number difference between G2 and G3.

In Figure S5, G1 and G2 exhibit negative height values which means that both areas are positioned lower than the silicon wafer substrate. We assume that a higher amount of adsorbates settled on the silicon wafer than on the graphene flake surface. After the first oxygen-plasma treatment of the few-layer graphene/graphite sample, the height values of areas G1 and G2 became positive. This indicates that both areas are situated higher than the silicon wafer substrate which could be explained by the higher amount of adsorbate removal from the silicon wafer than from the flake surface.

6. Stripe-like and island structure formation on few-layer graphene/graphite

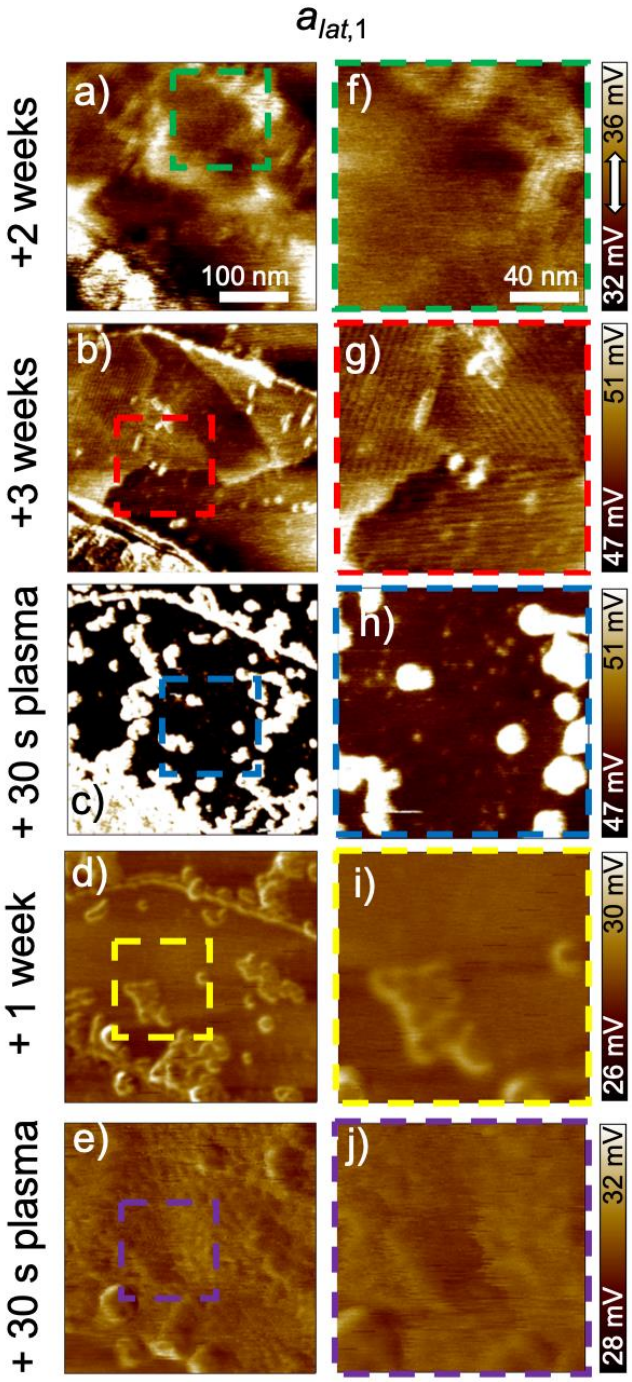

Figure S6: Stripe-like and island structure formation on a few-layer graphene/graphite flake analyzed based on the lateral drive amplitude images at two magnifications (a–e: 350 × 350 nm^2 and f–j: 150 × 150 nm^2) after different durations of storage and stepwise oxygen-plasma treatment in AMFlex2-OLTor1-FMLat1 AFM mode. $A_{0\ (flex,2)}$ = 675 nm, $A_{flex,2}$ = 600 nm and $A_{lat,1}$= 1.766 nm. The white arrow within the color bar (f) indicates the direction of lateral oscillation. The dashed squares in Figure S6a-e represent the zoom-in areas for the images shown in f-j. The same color of these squares represents the same storage or oxygen-plasma treatment step.

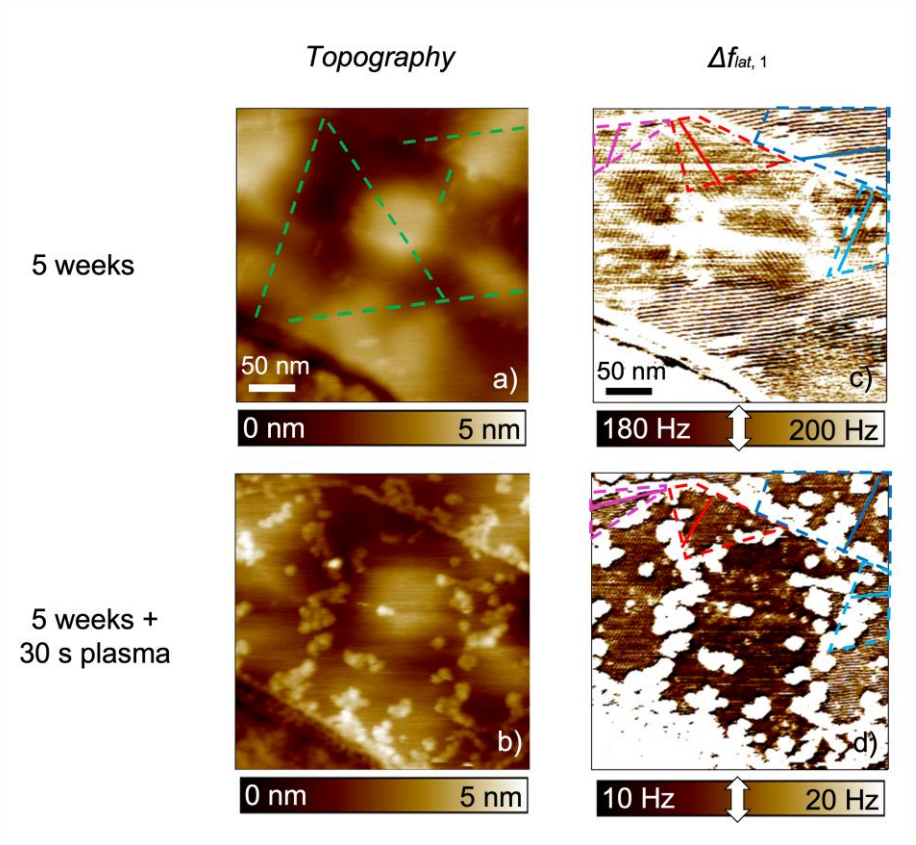

Figure S7: Stripe-like and island structure formation on a few-layer graphene/graphite flake analyzed based on the topographic and lateral frequency-shift images before (a, c) and after 30 s plasma treatment (b, d) in shielded configuration in AMFlex2-OLTor1-FMLat1 AFM mode. $A_{0\,(flex,2)}$ = 675 nm, $A_{flex,2}$ = 600 nm and $A_{lat,1}$= 1.766 nm. White arrows within the color bars indicate the direction of lateral oscillation. The green dashed lines visible in the topographic image recorded before the plasma treatment in (a) are a guide to the eye to highlight the different orientations of the stripe-like pattern. The different colored polygons with the included solid lines observable in the lateral frequency-shift images in (c) and (d) indicate the areas on the flake surface where a change in the orientation of the stripe pattern was caused by the oxygen-plasma treatment.

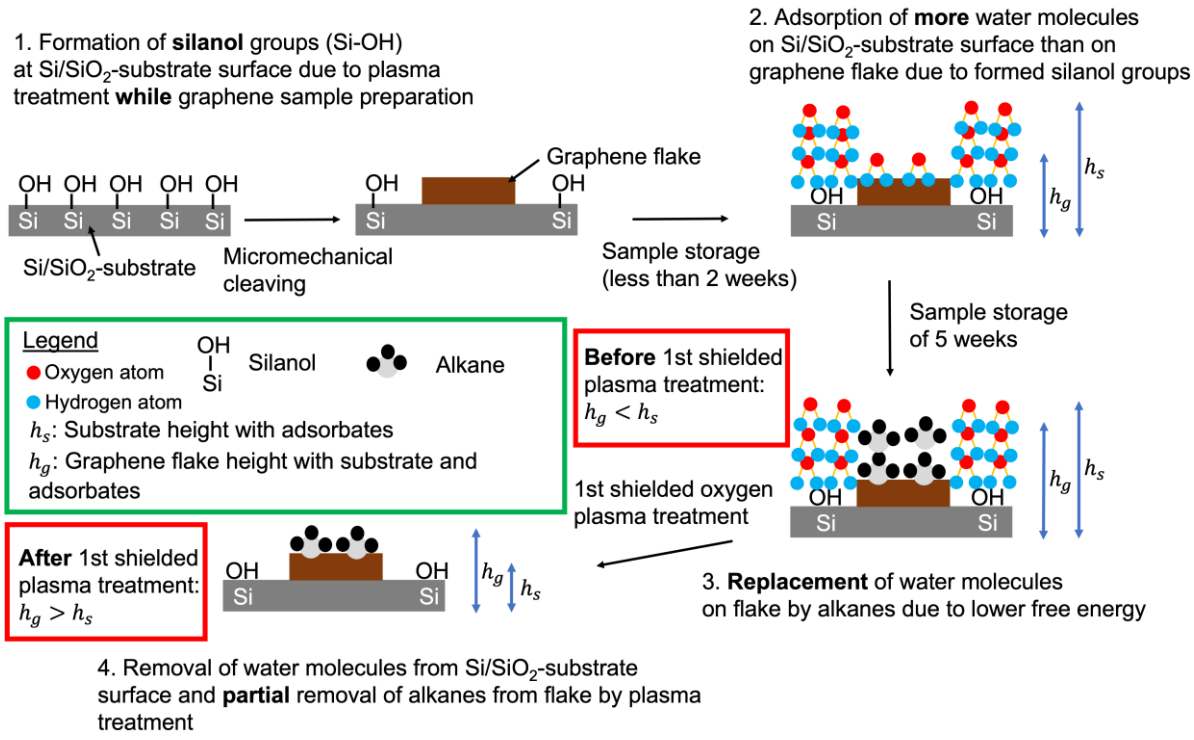

Figure S8: Scheme of the proposed height evolution and adsorbate removal upon graphene sample preparation and first shielded plasma treatment.

The scheme visualized in Figure S8 shows the fundamental processes behind the evolution of graphene and substrate height taking place upon sample preparation and the first shielded oxygen-plasma treatment. In the first step of the graphene sample preparation, the surface of the Si/SiO2-substrate was directly exposed to oxygen plasma to remove the organic contaminants. Consequently, silanol groups formed at the substrate surface by reaction of the silicon atoms with active oxygen species from the plasma and water molecules so that the surface got hydrophilic. In the last step of the sample preparation, the graphene flake was mechanically exfoliated and deposited onto the Si/SiO2-substrate. The storage of the graphene sample under ambient conditions led to a higher amount of water molecules being adsorbed on the substrate surface than on the graphene flake due to the higher hydrophilicity of the Si/SiO2-substrate caused by the formed silanol groups. This explains why in the amplitude modulation AFM measurements in Figure S2 and in the multifrequency AFM measurements shown in Figure S5 the Si/SiO2-substrate seems to exhibit a higher height than the actual graphene flake with the underlying substrate. With ongoing storage time of the graphene sample, the water molecules adsorbed on the graphene flake surface were replaced by the alkanes with 20-26 carbon atoms (stripe-like patterns in AFM measurements) due to their comparably lower free energy. At this stage, the substrate height with adsorbates was still higher than the graphene flake surface on the Si/SiO2-substrate carrying the adsorbates. The first shielded plasma

treatment caused a higher removal of the water molecules from the Si/SiO_2-substrate and only a partial removal of the long-chain alkanes from the substrate surface due to their high binding energies. Therefore, the height level of the graphene flake became higher than the Si/SiO_2-substrate level after the first oxygen-plasma treatment.

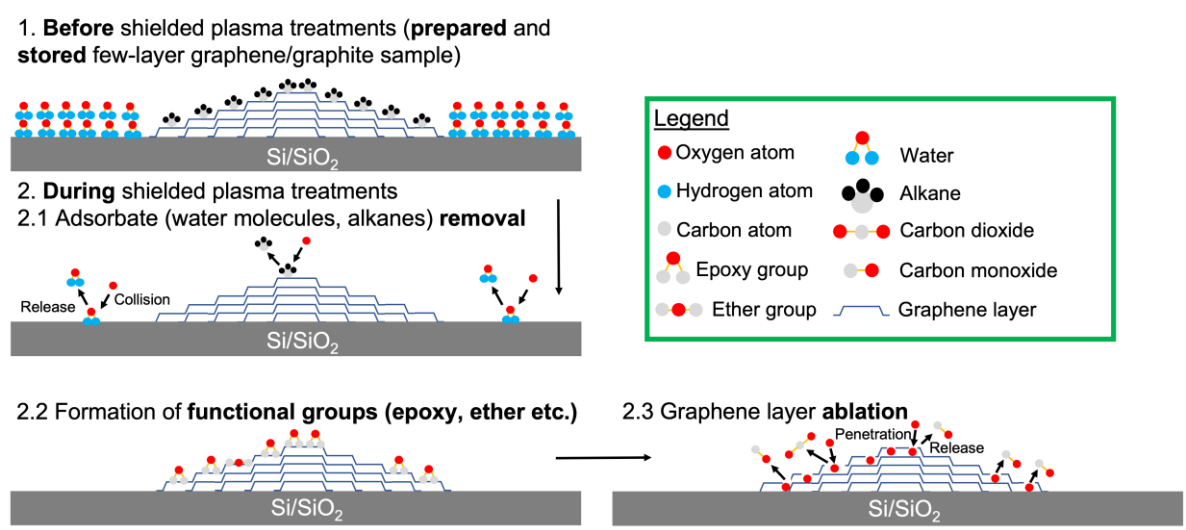

Figure S9: Schematic representation of adsorbate removal and graphene layer ablation during shielded oxygen-plasma treatment.

In Figure S9 the processes of adsorbate removal and graphene layer ablation are schematically depicted. In step 1 of this scheme, the few-layer graphene/graphite sample is shown after the sample preparation and the storage for a few hours or days under ambient conditions. Due to the storage, water molecules and alkanes adsorbed on the flake and Si/SiO_2-substrate surface. When the few-layer graphene/graphite sample was treated by oxygen plasma, the adsorbates were removed by interaction with active oxygen of the plasma from the surface of the graphene flake and the Si/SiO_2-substrate before ablation of the graphene layer started (see step 2.1 in Figure S9). After the adsorbate removal, in step 2.2 the oxygen atoms from the plasma could be incorporated into the graphene layers by forming functional groups, such as epoxy and ether groups. According to the scheme about the water island formation (see Figure 5 of the main text), vacancies were generated by transformation of the functional groups to CO and CO_2. These gaseous reaction products were released to the surrounding atmosphere. As a result, either water molecules filled the vacancies to assemble water islands or accumulation of vacancies up to a complete ablated graphene layer occurred.

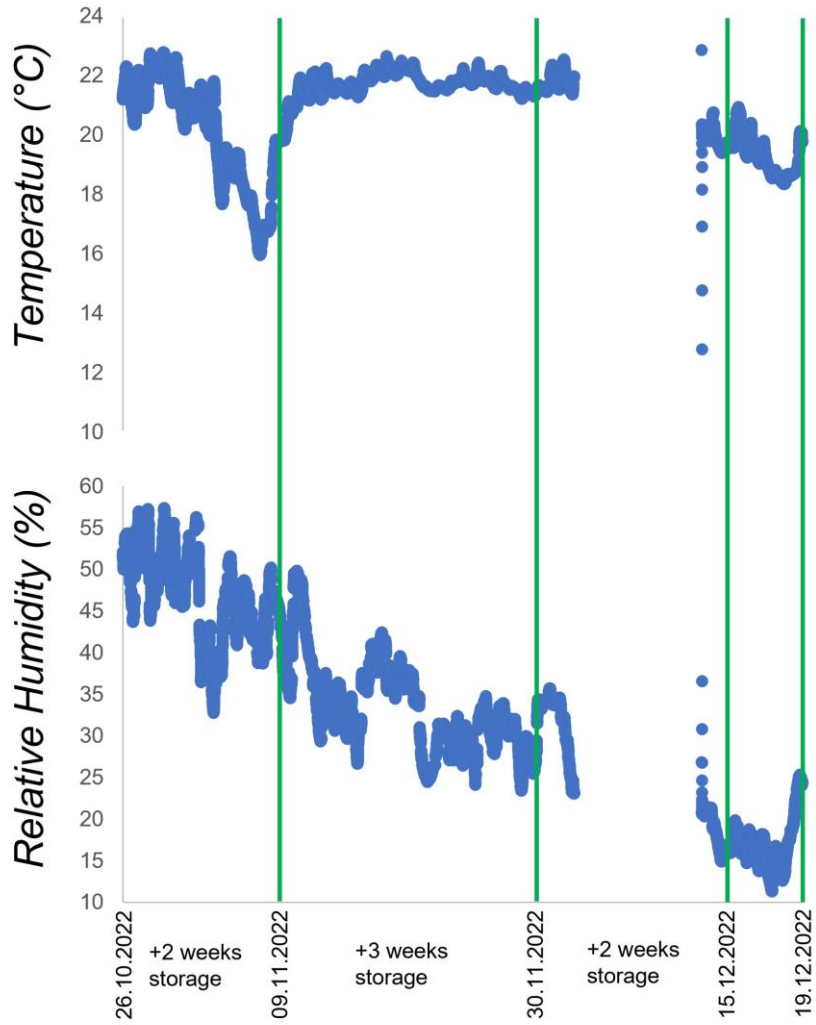

Figure S10: Temperature and relative humidity measured during storage of the few-layer graphene/graphite sample in a polypropylene box under laboratory air conditions.

References

1. Zandiatashbar, A., et al., Effect of defects on the intrinsic strength and stiffness of graphene. Nature Communications, 2014. 5: p. 3186.